Attachment-induced ionization instability in electronegative capacitive RF discharges

A Descoeudres, L Sansonnens and Ch Hollenstein

Centre de Recherches en Physique des Plasmas, Ecole Polytechnique Fédérale de Lausanne, CH-1015 Lausanne, Switzerland

E-mail: antoine.descoeudres@epfl.ch

Abstract. Attachment-induced ionization instability has been experimentally observed in O_2 and CF_4 capacitive RF discharges using time-resolved voltage probe, Langmuir probe, optical emission and mass spectrometry measurements. This instability occurs under specific conditions of power and pressure, and produces synchronized oscillations in the kHz range on potentials, emission intensity and positive ions fluxes. On the contrary, the SF_6 plasma was observed to remain stable under all experimental conditions. This can be understood by considering attachment and ionization cross sections of these gases and applying the theoretical criterion of instability. Contrary to O_2 and CF_4, the attachment rate coefficient of SF_6 is very high at low energy and has a negative dependence on the electronic temperature. The application of the criterion shows clearly that O_2 and CF_4 plasmas are unstable at low electronic temperature, and that the SF_6 plasma is stable due to its particular low-energy attachment cross section.

1. INTRODUCTION

Radio-frequency discharges in electronegative gases are widely used in industrial processes, particularly in the manufacturing of semiconductor devices. Oxygen (O_2), sulfur hexafluoride (SF_6) and carbon tetrafluoride (CF_4) are the main electronegative gases employed for etching applications [1]. Inductively coupled plasmas (ICP) are used for most electronic devices but capacitively coupled plasmas (CCP) remain the choice in large area applications such as thin film transistors for flat display.

The presence of negative ions in a discharge changes considerably the physics of the plasma. Especially, several instabilities linked with the electronegativity of the gas can develop. Ionization waves have been studied in SF_6 DC glows [2]. In DC glows of other electronegative gases such as CO_2, CO and O_2, the attachment-induced ionization instability has been observed [3, 4, 5] and described in detail in [5]. There are also instabilities in inductive RF discharges, e.g. in O_2 and SF_6 [6, 7]. In this case the instability is attributed to the transition between inductive and capacitive modes.

The attachment-induced ionization instability occurs in DC glow discharges but also in capacitively coupled RF discharges. The instability was first observed in O_2 capacitively

coupled RF plasmas [8] and was also modelled for CF_4 [9, 10]. Nevertheless, the experimental characterization of this phenomenon is incomplete. Particularly, the question of appearance of the instability in other electronegative gases is still open [8]. This can be important for processes that require stable plasma characteristics.
In this paper we present observations of the attachment-induced ionization instability in O_2 and CF_4 capacitively coupled plasmas. The instability appears as oscillations on all the diagnostics used. The experimental conditions under which the discharge is unstable are also investigated. In the discussion we present the mechanism of the instability and apply the theoretical instability criterion of Nighan and Wiegand [5]. This criterion explains another important experimental result, namely the stability of the SF_6 plasma. Combined with simulation results, the criterion can also predict the unstable plasma conditions of the discharge.

2. EXPERIMENTAL SETUP

The experimental apparatus shown in figure 1 is a parallel plate capacitively coupled reactor comprising two stainless steel cylindrical electrodes 13 cm in diameter with a 2.5 or 4 cm electrode gap (for more details, see [11]). The typical plasma parameters used were: gas pressure 0.1 - 0.4 mbar, gas flow 13 sccm in SF_6, 20 sccm in CF_4 and 50 sccm in O_2, power up to 100 W at 13.56 MHz excitation frequency. A low frequency (50 Hz - 1 kHz) square wave modulation was applied to the high frequency excitation. This modulation permitted the synchronization of the diagnostics, the measurements of the negative ions during the afterglow [11] and to differentiate between transient and steady-state phenomena.

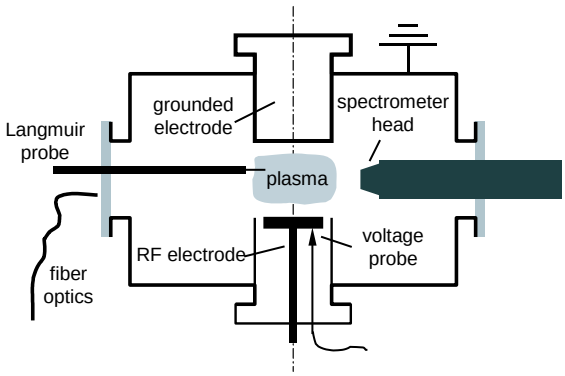

Figure 1. Schematic drawing of the reactor and diagnostics

For the characterization of the plasma, we used a voltage probe connected directly to the RF electrode to measure the external voltage envelope, and consequently the peak-to-peak voltage V_{pp} and the self-bias V_{sb}. The external envelope is the maximum and the minimum of the voltage measured at the RF electrode, averaged over a large number of low frequency modulation periods. A Scientific Systems Langmuir probe coupled to a

boxcar integrator was used to obtain time resolved current-voltage characteristics. The total plasma light was focused by a lens and collected with quartz fiber. We measured the global emission intensity with a Perkin Elmer C953 photomultiplier. The voltage and emission intensity data were recorded with a LeCroy digital oscilloscope. Finally, we used a Balzers PPM422 mass spectrometer combined with a EG&G Ortec multi channel scaler to obtain time-resolved ion flux measurements. The extraction head was biased to +5 V to collect a sufficient number of negative ions, no biasing was used when measuring the positive ions.

3. OBSERVATIONS OF THE INSTABILITY

An instability was observed both in O_2 and CF_4 discharges. The instability is not caused by external circuit effects, as we observed it in two different RF reactors, with two different RF matchboxes and amplifiers. The instability behaves in the same general way in these two plasmas. On the contrary, SF_6 discharges remain stable in all experimental conditions.

Oscillations are seen on the external voltage envelope. These oscillations develop under specific conditions of power and pressure. Figures 2 and 3 show voltage envelopes in O_2 discharges as a function of V_{pp} and pressure respectively. The threshold values of the unstable zone are different in O_2 and CF_4, but both plasmas behave generally in the same way. At low power the discharge is stable, becomes unstable with increasing power, and is stable again at high RF power. At 0.25 mbar, the instability occurs for applied peak-to-peak voltage between 185 V and 480 V in O_2 discharges, and between 220 V and 550 V in CF_4 discharges. A pressure threshold was also observed for the appearance of the instability. The plasma remains stable below 0.195 mbar in O_2 and 0.1 mbar in CF_4 at V_{pp} 250 V. Our measurements of the unstable zone for O_2 plasma are in good agreement with the results of Katsch *et al* [8], who found the unstable zone around 0.3 mbar and 300 V. We observed that the inter-electrode gap and gas flux have no influence on the presence of the instability.

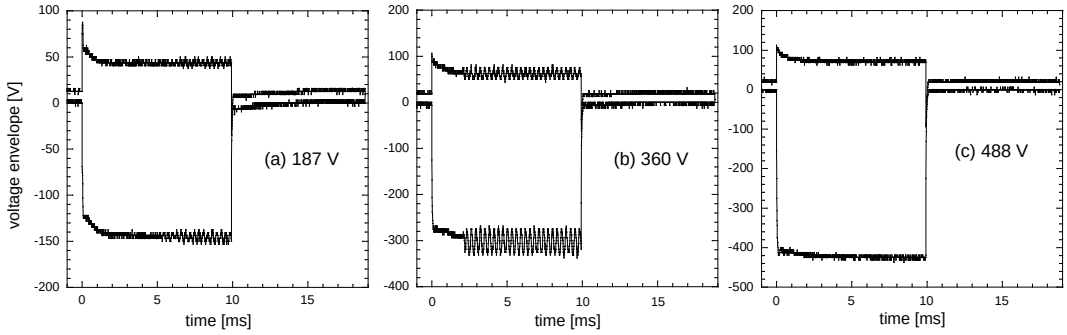

Figure 2. Instability on voltage envelope in O_2 plasma as a function of V_{pp} (0.25 mbar, 50 Hz modulation) : (a) 187 V (b) 360 V (c) 488 V

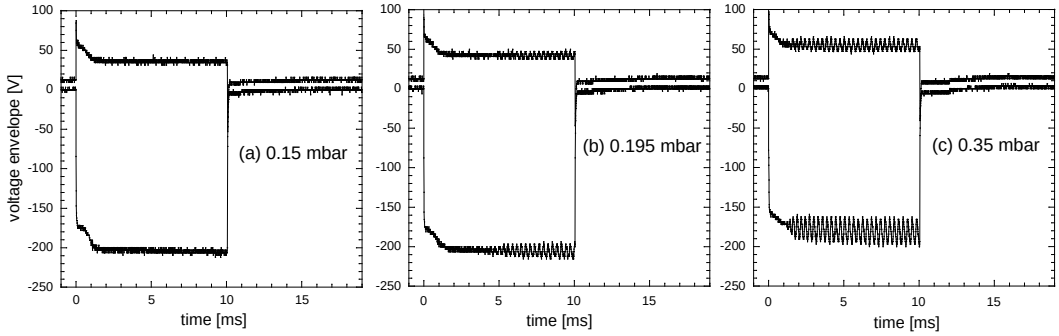

Figure 3. Instability on voltage envelope in O_2 plasma as a function of pressure (250 V V_{pp}, 50 Hz modulation) : (a) 0.15 mbar (b) 0.195 mbar (c) 0.35 mbar

We see in figures 2 and 3 that it takes a few ms for the oscillations to appear, and then they remain constant. The frequency of the oscillations is in the kHz range: 3.5 kHz in O_2 (consistent with results of [8]) and around 80 kHz in CF_4 at 0.25 mbar. In fact, the instability can also be observed without power modulation (continuous wave discharge). Since the voltage envelopes measurements are averaged over many low frequency square wave cycles, the instability is a very reproducible and regular phenomenon.

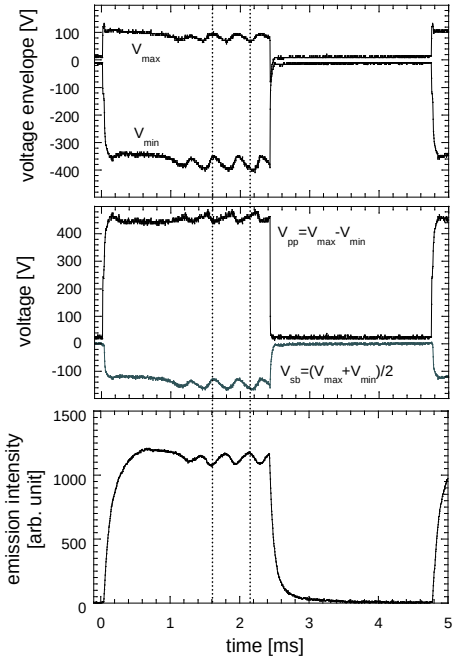

Figure 4. Instability on voltage envelope along with peak-to-peak voltage, self-bias voltage and global emission intensity in O_2 plasma (0.25 mbar, 450 V V_{pp}, 210 Hz modulation)

The different diagnostics show that many physical properties of the plasma follow the oscillations observed on voltage envelopes. Figure 4 shows variations of V_{pp}, V_{sb} and of the global emission intensity in a O_2 plasma. The fluxes of the positive ions CF_3^+ in pure

CF_4 plasma and O_2^+ in pure O_2 plasma at various energies are also affected, as shown in figure 5. The voltage oscillations, emission intensity and the ion fluxes were perfectly synchronized. Finally, the Langmuir probe results seem to show oscillations on the floating potential V_f, plasma potential and electronic saturation current, as Katsch *et al* reported it for oxygen [8]. We verified that the floating potential was really oscillating by connecting the Langmuir probe (without bias) directly to the oscilloscope.

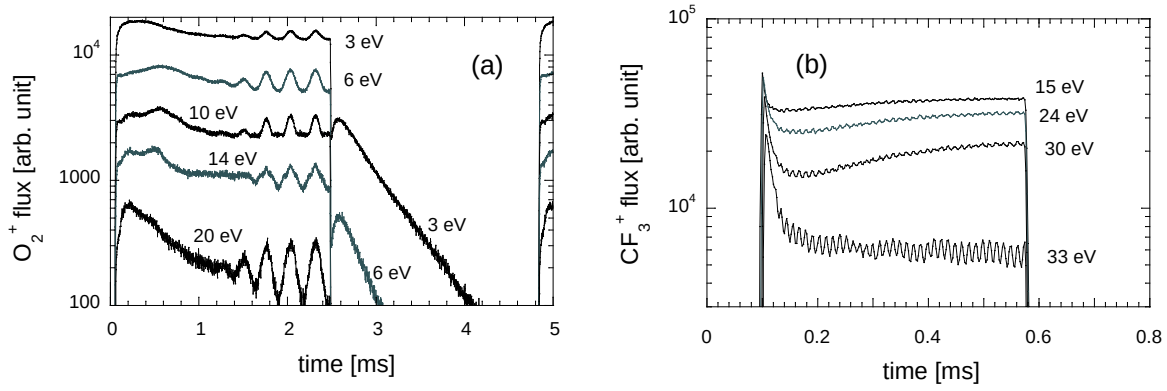

Figure 5. Instability on fluxes of positive ions (a) O_2^+ (0.25 mbar, 230 V V_{pp}, 210 Hz modulation) and (b) CF_3^+ (0.25 mbar, 200 V V_{pp}, 1 kHz modulation)

The amplitude of the oscillations in diluted Ar + CF_4 and Ar + O_2 discharges decreases with increasing concentrations of argon at fixed power and pressure. In Ar + CF_4 discharges for example, the negative ion flux and the amplitude of the oscillations decrease strongly above 80% of argon. This indicates that negative ions play a crucial part in the development of this type of instability.

4. DISCUSSION

The oscillations described previously can be attributed to the attachment-induced ionization instability. The instability mechanism is described in detail by Nigham and Wiegand [5] and can be summarized as follows.

Let us assume a small initial increase in the electronic density n_e. This will generally be followed by a decrease in the electronic temperature T_e due to the quasi-steady nature of the electron energy response [5]. This diminution of T_e has different consequences according to the nature of the gas.

In electropositive plasmas, electrons and positive ions are created by ionization and lost mainly by diffusion to the walls and recombination. Ionization decreases if T_e is diminished. Thus the electronic density decreases in response to the initial increase in n_e. This negative feedback stabilizes the perturbation.

In electronegative plasmas, electrons are also lost by attachment, and the efficiency of this process depends on electronic temperature. If the attachment decreases less strongly than the ionization decreases with the diminution of T_e, the electronic density

will decrease and the perturbation is stabilized. But in certain electronegative gases, the attachment can decrease more strongly than the decrease in ionization if T_e decreases. In this case, the decrease of T_e following an increase in n_e will cause a further increase of n_e (positive feedback), and the discharge becomes unstable. In this type of instability, n_e and T_e are the physical values that are the source of the oscillations. Their variations lead to changes in the other measured quantities such as the ions fluxes, the emission intensity and the electrical potentials (V_{pp}, V_{sb}, V_f, V_p). The plasma must reach certain conditions of n_e and T_e before the instability can develop. This is the cause of the delay of few ms observed.

This general description has been expressed by a necessary condition for the appearance of the instability by Nigham and Wiegand [5]. The physical basis of this criterion are the conservation equations of electronic and ionic densities. The plasma can be unstable if

$$R \doteq \frac{\partial k_a/\partial T_e}{\partial k_i/\partial T_e} > 1 \tag{1}$$

where k_a is the attachment rate coefficient and k_i the ionization rate coefficient. The rate coefficient k_j of the process j is defined by

$$k_j \doteq \sqrt{\frac{2e}{m_e}} \int_0^\infty \sigma_j(E) \cdot f(E) \cdot E \cdot \mathrm{d}E \tag{2}$$

where E is the energy of the colliding electron, charge e and mass m_e, f the energy distribution and σ_j the cross section of the process.

Since the electron energy distribution and thus the rate coefficients k_j are functions of T_e, the ratio R depends on T_e also. In practice, the criterion (1) is fulfilled if the attachment rate coefficient increases with electronic temperature faster than the ionization rate. From a detailed analysis of the electron continuity equation, Nighan and Wiegand also deduce that the negative ion density has to be of the same order as the electron density, otherwise the perturbation is stabilized [5]. In fact the instability involves coupled fluctuations of both negative populations.

For the calculation of the integrals (2), we use the attachment and ionization cross sections shown in figure 6, given in [12, 13, 14, 15]. For the electron energy distributions, we used solutions of the Boltzmann equation calculated with Bolsig from Kinema Software [16]. The calculated distribution remains close to the Maxwellian distribution, and therefore we use the associated Maxwellian electron temperature in the following discussion. Calculated attachment and ionization rate coefficients for O_2, CF_4 and SF_6 are shown in figure 7, and the ratio R in figure 8.

The ionization cross sections and therefore the ionization rate coefficients are quite similar for the three gases. As mentioned above, the ionization rate coefficient decreases with a diminution of the electronic temperature (k_i is an increasing function of T_e). But SF_6 differs from O_2 and CF_4 by its attachment cross section. The calculations of R in figure 8 demonstrate that O_2 and CF_4 plasmas can be unstable at low electronic temperature (under 3.9 eV and 5.05 eV respectively). These gases have such properties

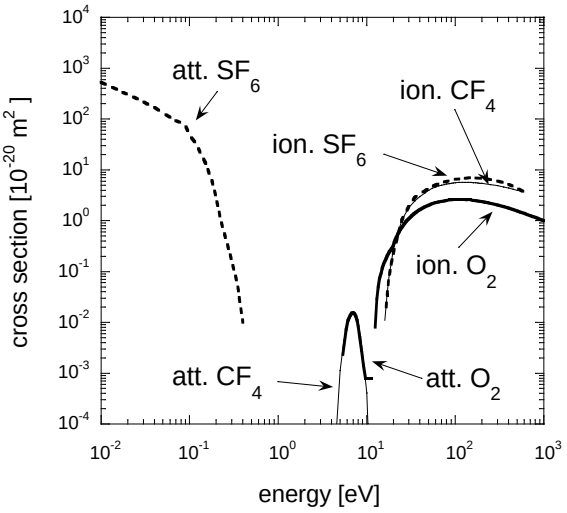

Figure 6. Attachment and ionization cross sections for O_2 [12], CF_4 [13, 14] and SF_6 [15]

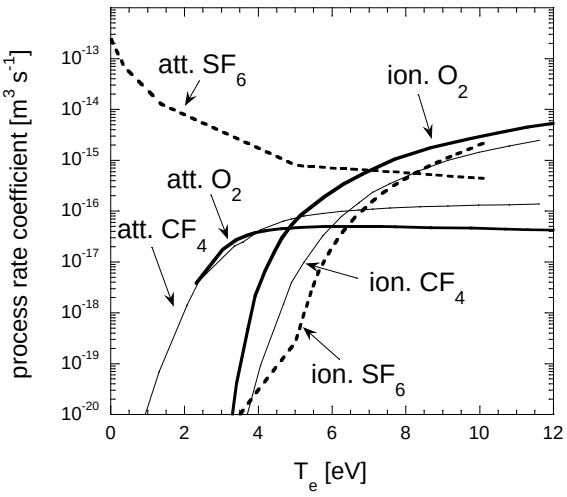

Figure 7. Calculations of attachment and ionization rate coefficients for O_2, CF_4 and SF_6

that the two instability conditions described previously can be satisfied. On the contrary, SF_6 plasma always remains stable. The attachment is much more effective in particular for low energy electrons, which are dominant by far. This particular attachment cross section results in low electronic density, experimentally confirmed by a very weak plasma luminosity and a low self-bias (only a few volts). Furthermore, the attachment rate coefficient decreases with T_e, which is why R is negative at any electronic temperature. The attachment cross section is the source of the strong electronegativity and leads to the stability of SF_6 discharges.

Knowing the corresponding attachment and ionization cross sections, this approach can be applied to other electronegative gases used in industry. For example, the cross

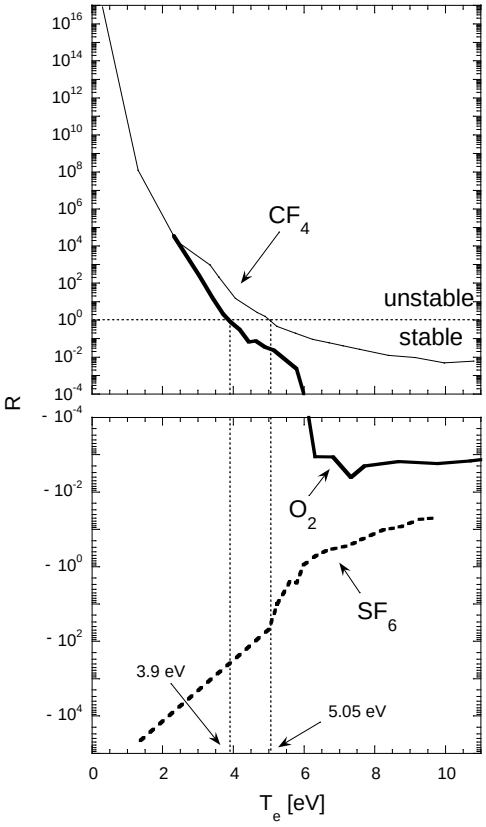

Figure 8. Instability criterion: calculation of the ratio R for O_2, CF_4 and SF_6. The plasma can be unstable if T_e is lower than 3.9 eV in O_2, 5 eV in CF_4

sections of C_2F_6 [14, 17], C_3F_8 [14, 18] and Cl_2 [19] indicate that these plasmas can be unstable, whereas CCl_2F_2 [20] and CF_3I [21] plasmas should remain stable. This remains to be confirmed experimentally.

Once the threshold temperature at which $R = 1$ is known, a discharge simulation is useful to calculate the corresponding pressure and power conditions. These conditions can be compared with our experimental zones of instability. To simulate the discharge, we use Siglo-RF from Kinema Software [22], a fluid model solver. The discharges are certainly more complicated than those predicted by this model, but simulations give interesting qualitative informations. The chosen plasma parameters are the same as in our experiments. Figure 9 shows computation of T_e as a function of pressure (at V_{pp} 250 V) and figure 10 shows T_e as a function of V_{pp} (at 0.25 mbar) for O_2 and CF_4.

At 250 V, the simulation predicts unstability over 0.175 mbar in CF_4 (experimentally 0.1 mbar), and over 0.3 mbar in O_2 (experimentally 0.195 mbar). Although the threshold pressures do not match exactly, the computed dependence of T_e with the pressure is in good agreement with our results. The temperature decreases with increasing pressure, leading to stability of the discharge at low pressure. In practice, the attachment-induced ionization instability should not be a problem for etching applications, which are carried out at low pressure.

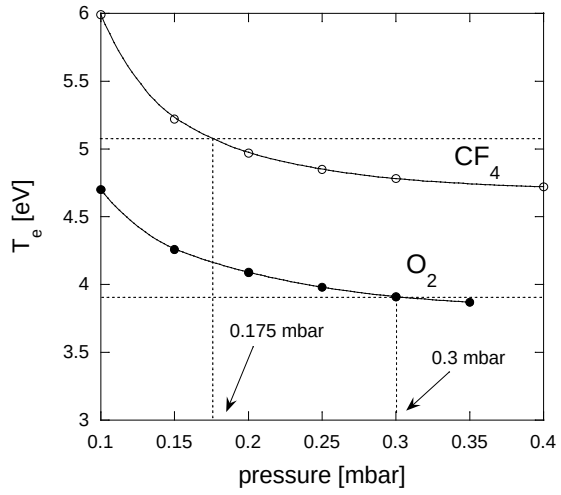

Figure 9. Electronic temperature vs pressure in O_2 and CF_4 calculated with Siglo-RF (250 V V_{pp}). According to figure 8, the simulation predicts unstability over 0.175 mbar in CF_4 and over 0.3 mbar in O_2

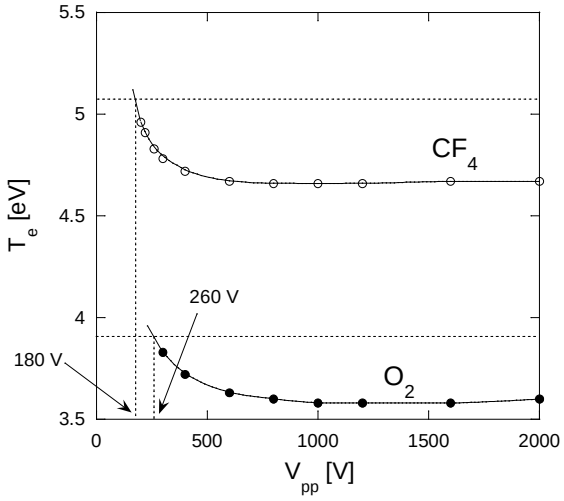

Figure 10. Electronic temperature vs RF voltage in O_2 and CF_4 calculated with Siglo-RF (0.25 mbar). According to figure 8, the simulation predicts instability above 180 V in CF_4 and above 260 V in O_2

At 0.25 mbar, the computed zone of instability begins at 180 V in CF_4 (experimentally between 220 and 550 V), and at 260 V in O_2 (experimentally between 185 and 490 V). The lower thresholds are again not so far from our measurements. But the simulation does not predict an upper threshold as we measure it. In any case, the calculated temperature increase slightly at high power, but insufficiently to overcome 3.9 eV and 5.05 eV in O_2 and CF_4 respectively.

5. CONCLUSION

The attachment-induced ionization instability occurs in O_2 and CF_4 capacitively coupled RF discharges under specific conditions of power and pressure, but not in SF_6. The instability is experimentally observed through oscillations in the kHz range on electrical potentials (V_{pp}, V_{sb}, V_f and V_p), emission intensity and positive ion flux measurements. We also have obtained an experimental proof of the correlation between the instability and negative ions, with the measurements in diluted Ar + CF_4 and Ar + O_2 discharges. The cause of all these oscillations is coupled variations of n_e and T_e. If the attachment rate coefficient increases more strongly than the ionization rate coefficient with T_e and if electronic and negative ions densities are of the same order of magnitude, a small increase in n_e can rapidly grow via a decrease in T_e. The plasma becomes unstable, and electronic and negative ions densities increase alternately.

SF_6 differs from O_2 and CF_4 by its very high attachment cross section at low energy and by the negative dependence of this attachment rate coefficient. This results in strong electronegativity and stability of SF_6 discharges. This experimental result is confirmed by the application of the theoretical instability criterion.

Simulation results confirm that the O_2 and CF_4 discharges are stable at low pressure and low power, because of a high electronic temperature. The calculated thresholds values are of the same order of magnitude as the experimental measurements, but the criterion gives a rather qualitative indication of plasma stability. It is difficult to determine precisely the unstable zone in terms of power and pressure by calculation. Nevertheless, this criterion can be applied to other electronegative gases if the ionization and attachment cross sections are known.

References

[1] Lieberman M A and Lichtenberg A J 1994 *Principles of plasma discharges and materials processing* (New York: Wiley)

[2] Ishikawa I, Matsumoto M and Suganomata S 1984 *J. Phys. D: Appl. Phys.* **17** 85

[3] Haas R A 1973 *Phys. Rev. A* **8** 1017

[4] Nighan W L, Wiegand W J and Haas R A 1973 *Appl. Phys. Let.* **22** 579

[5] Nighan W L and Wiegand W J 1974 *Phys. Rev. A* **10** 922

[6] Tuszewski M 1996 *J. Appl. Phys.* **79** 8967

[7] Chabert P, Lichtenberg A J, Lieberman M A and Marakhtanov A M 2001 *Plasma Sources Sci. Technol.* **10** 478

[8] Katsch HM, Goehlich A, Kawetzki T, Quandt E and Döbele HF 1999 *Appl. Phys. Let.* **75** 2023

[9] Gogolides E, Stathakopoulos M and Boudouvis A 1994 *J. Phys. D: Appl. Phys.* **27** 1878

[10] Metsi E, Gogolides E and Boudouvis A 1996 *Phys. Rev. E* **54** 782

[11] Howling A A, Sansonnens L, Dorier J-L and Hollenstein C 1994 *J. Appl. Phys.* **75** 1340

[12] Lawton S A and Phelps A V 1978 *J. Chem. Phys.* **69** 1055

[13] Christophorou L G, Olthoff J K and Rao M V V S 1996 *J. Phys. Chem. Ref. Data* **25** 1341

[14] Christophorou L G and Olthoff J K 1999 *J. Phys. Chem. Ref. Data* **28** 967

[15] Christophorou L G and Olthoff J K 2000 *J. Phys. Chem. Ref. Data* **29** 267

[16] Pitchford L C, O'Neil S V and Rumble J R 1981 *Phys. Rev. A* **23** 294

[17] Christophorou L G and Olthoff J K 1998 *J. Phys. Chem. Ref. Data* **27** 1

[18] Christophorou L G and Olthoff J K 1998 *J. Phys. Chem. Ref. Data* **27** 889
[19] Christophorou L G and Olthoff J K 1999 *J. Phys. Chem. Ref. Data* **28** 131
[20] Christophorou L G, Olthoff J K and Wang Y 1997 *J. Phys. Chem. Ref. Data* **26** 1205
[21] Christophorou L G and Olthoff J K 2000 *J. Phys. Chem. Ref. Data* **29** 553
[22] Boeuf J-P and Pitchford L C 1995 *Phys. Rev. E* **51** 1376